Experimental validation of thermal model of hybrid photovoltaic thermal (HPVT) double slope active solar still

Gajendra Singh[a], V.K. Dwivedi[b,*], J.K. Yadav[b], G.N. Tiwari[c]

[a]Department of Electrical Engineering, Krishna Institute of Engineering and Technology, Meerut Road, Ghaziabad, Uttar Pradesh 201206, India
[b]Department of Mechanical Engineering, Galgotias College of Engineering and Technology, 1, Knowledge Park-II, Greater Noida, Uttar Pradesh-201306, India
Tel. +91 9953001761; Fax: +91 01232262060; email: vkdwivedi94@gmail.com
[c]Centre for Energy Studies, Indian Institute of Technology, Delhi, Hauz Khas, New Delhi-110016, India

ABSTRACT

A HPVT double slope active solar still was designed and fabricated to study their performance. In this paper thermal modeling of HPVT double slope active solar still with two flat plate collectors connected to the basin of solar still has been carried out. Analytical expressions for yield, water temperature and condensing cover temperature have been derived as a function of climatic and design parameters on the basis of energy balance equations. The thermal model of distillation system has been validated with experimental data. It has been established that there are close agreement between theoretical and experimental results with coefficient of correlation varying from 0.872 to 0.965.

Keywords: Solar distillation; Thermal modeling; Heat and mass transfer

1. Introduction

The world population is increasing rapidly. The population growth coupled with industrialization and urbanization will result in an increasing demand for water and will have serious consequences on the environment. In order to cater the demand of water purification rigorous researches have been carried out by scientists on design, fabrication and development of solar stills. Dwivedi and Tiwari [1] have carried out mathematical modeling of double slope passive and active type of solar still. Kumar and Tiwari [2] carried out life cycle cost analysis of single slope hybrid (PV/T)

active solar still. Rubio et al. [3] proposed a new mathematical model to study the performance of a double slope passive solar still by considering the effect of heat capacity of condensing covers and bottom insulation. Tiwari and Tiwari [4] have conducted experiment for performance analysis and thermal modeling of single slope passive solar still for different inclination of condensing covers. Tanaka et al. [5] developed a highly productive basin type-multiple effects coupled solar still generally known as active solar still. Tripathi and Tiwari [6] conducted outdoor experiments to study the effect of water depth on internal heat and mass transfer for active solar distillation systems. Recently, Tiwari et al. [7] have studied the comparative performance evaluation of an active solar distillation system and tried to evaluate

*Corresponding author.

theoretical yield from the active solar stills integrated with FPC, concentrating collector, evacuated tube collector with and without heat pipe. The passive solar distillation system is a slow process for purification of saline/brackish water. When flat plate collector is integrated with solar still, extra thermal energy is supplied to the basin water and hence rise in water temperature is more as compared to passive solar still as reported by Dwivedi and Tiwari [8]. Hayek and Badran [9] studied the effect of using different designs of solar stills on water distillation. OO and Al-Tahaineh [10] studied the effect of coupling flat plate collector on the solar still productivity. Rubio et al. [11] studied Cavity geometry influence on mass flow rate for single and double slope solar stills. Kumar and Tiwari [12] evaluated the Life cycle cost analysis of single slope hybrid (PV/T) active solar still. Comparison of internal heat transfer coefficients in passive solar stills by different thermal models were carried out by Dwivedi and Tiwari [13]. Dev and Tiwari [14] derived characteristic equation of a hybrid (PV-T) active solar still whereas characteristic equation for double slope passive solar still were derived by Dev et al. [15]. A detailed review of solar stills has been done by Dev and Tiwari [16].

In this paper, thermal model for a new design of hybrid photovoltaic thermal (HPVT) double slope active solar still have been derived on the basis of energy balance for different components of solar still and two flat plate collectors. Thermal validation is carried out from the experimental data obtained under field conditions.

2. Design description of experimental setup and its working principle

The schematic diagram and photograph of fabricated HPVT double slope active solar still are shown in Figs. 1a and 1b respectively. To increase the temperature of feed water in the solar still, the double slope solar still is
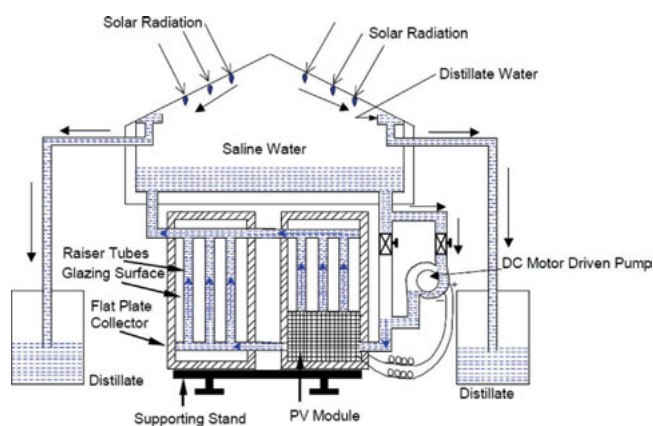

Fig. 1b. Photograph of HPVT double slope active solar still.

connected to the two flat plate collectors with one of them is photovoltaic (PV) integrated. The flat plate collectors make an angle of 30° with horizontal, optimized for 28.45° N latitude of Ghaziabad (India). The fabricated system consists of four components namely double slope still, PV integrated flat plate collectors, DC water pump and connecting insulated pipe. Single basin double slope solar still of basin area 2.0 m × 1.0 m was fabricated using fiber reinforced plastic (FRP) of low thermal conductivity. The thickness of FRP to prepare the walls and basin of solar still was 0.005 m. The lower wall height facing East and West (E-W) directions has been kept 0.22 m.

Interior of the basin is painted black with dye to increase the absorptivity to solar radiations. The top of the basin is covered each side with glass of thickness 0.004 m, inclined at 15° and oriented to due E-W direction respectively, to receive the maximum possible solar radiation. The rubber gasket is placed in between glass cover and top of the basin of solar still. Further, it is sealed using window putty to prevent vapor leakage. The condensed water is collected in a galvanized iron channel fixed at the lower end side of both the glass covers. The distillate collected is continuously drained through flexible pipe and stored in a jar placed outside on both sides. In an active solar still, the water in the basin gets heated directly as well as indirectly through flat plate collectors.

Two flat plate collectors are connected together and integrated to the basin of solar still by using insulated pipes (insulated using thick rubber coating). The connections between the two flat plate collectors are in parallel as shown in Fig. 1a. Each collector has an effective area of 2.0 m². The whole absorber is encased in an aluminum metallic box with 0.1 m glass wool insulation

Fig. 1a. Schematic diagram of HPVT double slope active solar still.

at base and side to reduce thermal losses. The toughened glasses of 0.004 m thick are fixed on the top of the boxes using aluminum frame and screw. The rubber seal is placed between the metallic box and glass cover as well as between glass and aluminum frame. A glass to glass PV module of 36 cells (40 Wp) has been integrated at the bottom of one of the collector. The size of module is kept 0.55×1.25 m^2. The solar radiations pass through the non-packing area of the module as well as convected energy from back side of the module is utilized to heat the water flowing through the riser tubes below the module. The whole system is made vapor tight using silicone rubber sealant, as it remains elastic for long time.

The DC water pump of size 40 W is used to circulate the water in forced mode of operation. The pump is driven directly by the DC power generated by the PV module. The specification of the experimental system is given in the Table 1. The pump operates only during sunshine hour, to avoid reverse heat flow from water during off sunshine hours.

3. Instrumentation

The following instruments have been used during the experimentation for measuring the various parameters:

1. Copper constantan thermocouples: These thermocouples have been used to measure the temperature of water, vapor and condensing cover using a digital temperature indicator having a least count of 0.1°C and it can measure temperature in the range of −10°C–300°C. The thermocouples used in the experimental work have been calibrated with the help of standard zeal thermometer. To measure water temperature thermocouples have been submersed inside the water whereas for measuring condensing cover temperature thermocouples were pasted on inner and outer surfaces with the help of araldite. For measuring vapor temperature thermocouples have been hanged in between water surface and glass covers.
2. Mercury thermometer: A Calibrated mercury thermometer of least count 1°C has been used to record the ambient air temperature. The thermometer has been kept to the height of the solar still under shade to prevent direct exposure to the radiations. The range of thermometer used was 0–100°C.
3. Solarimeter: A calibrated solarimeter (with the help of a Pyranometer) has been used to measure the total as well as diffuse solar radiations. It has least count of 2 mW cm^{-2}. The Solarimeter has been manufactured by Central Electronics Limited Sahibabad, UP, India. It can measure solar radiation up to 1200 W m^{-2}.
4. Measuring cylinder: The collected distillate yield has been measured using graduated cylinder with least count of 1 ml.

Table 1
Specifications of fabricated HPVT double slope active solar still

Component	Specifications
Flat plate collectors	
Collector type	Tube in plate type
No of collectors	2
Area of each collector (effective)	2.00 m^2
Tube material	Copper tubes
Plate thickness	0.002 m
Riser – outer diameter	0.0127 m
Riser thickness	0.56×10^{-3} m
Spacing between two risers	0.112 m
Thickness of insulation	0.1 m
Weight of the collector	48 kg
Angle of collectors	30°
Thickness of top glass	0.004 m
PV Module	
Size of PV module	1.25 m × 0.55 m
No of solar cells	36
Area of solar cell	0.008 m^2
Packing factor	0.44
Max power rating P_{max}	40 W
Motor used for water pump	DC shunt motor (18 V, 40 W and 2800 rpm)
Solar still	
Length	2 m
Width	1 m
Lower height	0.22 m
Higher height	0.48 m
Thickness of glass cover	0.004 m

4. Experimental procedure

Experiments have been performed to evaluate the performance of the solar still under the field conditions. 24 h before the commencement of test, the basin was filled with brackish water to a desired level (0.025 m) to bring the water in steady state. All the glass covers were cleaned for the dust/dirt particles before the experimentation. The tests started at 7:00 a.m. and continued till 7:00 a.m. on the next day. During experiment the following parameters were measured hourly.

(a) Solar intensities on E-W glass covers (b) solar intensities on collector panels (c) ambient air temperature

(d) basin liner temperature (e) water temperature inside still (f) vapor temperature inside still (g) inner surface temperature of glass covers (h) outer surface temperature of glass covers (i) hourly yields from E-W cover sides.

5. Thermal modeling

Following assumptions have been considered for writing energy balance equations for different components of a HPVT double slope active solar still:

1. The system is under quasi-steady state condition.
2. Thermal capacity of condensing covers and insulating material of wall of solar still has been neglected.
3. The connecting pipes between the solar still and flat plate collector are perfectly insulated.
4. There is no temperature gradient in the water inside the basin.
5. The average temperature of water column in the basin is equal to the average temperature of water in upper and lower header of flat plate collector.

5.1. Energy balance equation on inner surface of east condensing cover

$$\alpha'_g I_s(t)_E A_{gE} + h_{1wE} A_b \left(T_w - T_{giE}\right) - U_{EW} A_{gE} \left(T_{giE} - T_{giW}\right)$$
$$= h_{kg} A_{gE} \left(T_{giE} - T_{goE}\right) \tag{1}$$

where, $h_{kg} = k_g / l_g$.

5.2. Energy balance equation on outer surface of east condensing cover

$$h_{kg} A_{gE} \left(T_{giE} - T_{goE}\right) = h_o A_{gE} \left(T_{goE} - T_a\right) \tag{2}$$

5.3. Energy balance equation on inner surface of west condensing cover

$$\alpha'_g I_s(t)_W A_{gW} + h_{1wW} A_b \left(T_w - T_{giW}\right)$$
$$- U_{EW} A_{gW} \left(T_{giE} - T_{giW}\right) = h_{kg} A_{gW} \left(T_{giW} - T_{goW}\right) \tag{3}$$

5.4. Energy balance equation on outer surface of west condensing cover

$$h_{kg} A_{gW} \left(T_{giW} - T_{goW}\right) = h_o A_{gW} \left(T_{goW} - T_a\right) \tag{4}$$

5.5. Energy balance equation for basin Liner

$$\alpha'_b \left\{I_s(t)_E + I_s(t)_W\right\} A_b = h_{bw} A_b \left(T_b - T_w\right)$$
$$+ h_{ba} A_b \left(T_b - T_a\right) \tag{5}$$

5.6. Energy balance equation for water mass

$$\alpha'_w \left\{I_s(t)_E + I_s(t)_W\right\} A_b + h_{bw} A_b \left(T_b - T_w\right) + \dot{q}_u$$
$$= (MC)_w \frac{dT_w}{dt} + h_{1wE} A_b \left(T_w - T_{giE}\right)$$
$$+ h_{1wW} A_b \left(T_w - T_{giW}\right) + h_s A_s \left(T_w - T_a\right) \tag{6}$$

where

$$\dot{q}_u = A_C F' \left[(\alpha\tau) I_C - U_L (T_W - T_a)\right]$$

From above equations, one can get the following first order differential equation:

$$\frac{dT_w}{dt} + a T_w = f(t) \tag{7}$$

where

$$a = \frac{\left\{\dfrac{h_{bw}.h_{ba}.A_b}{h_{bw} + h_{ba}} + \dfrac{h_{1wE}.(p - A_2).A_b + h_{1wW}.(p - B_2).A_b}{p} + h_s.A_s\right\}}{(MC)_w} \tag{8}$$

and

$$f(t) = \frac{1}{(MC)_w} \begin{bmatrix} \left[\left(\dfrac{\alpha'_b h_{bw}}{h_{bw} + h_{ba}}\right) A_b \left(I_s(t)_E + I_s(t)_W\right)\right] \\ + \left(\dfrac{h_{bw} h_{ba}}{h_{bw} + h_{ba}} \times A_b + h_s A_s\right) \\ T_a \left(\dfrac{\left(h_{1wE} A_1 + h_{1wW} B_1\right) A_b}{P}\right) \\ + A_C F'(\alpha\tau) I_C + A_C F' U_L T_a \end{bmatrix} \tag{9}$$

The expressions for p, A_1, A_2, B_1, B_2, R_1, R_2, U_1, U_2 etc. have been given in Appendix-1 whereas the heat transfer relationship used in thermal modeling are given in given in the Appendix-2.

In order to obtain an approximate solution of Eq. (7) the following assumptions have been made:

1. The time interval Δt ($0 < t < \Delta t$) is small.
2. The function $f(t)$ is constant, that is, $f(t) = \overline{f(t)}$ for the time interval Δt.
3. 'a' is constant during the time interval Δt.

4. The internal convective (h_{cw}), evaporative (h_{ew}) and radiative (h_{rw}) heat transfer coefficients for E-W condensing cover have been evaluated at initial ($t = 0$) water (T_{w0}) and inner condensing cover (T_{gi0}) temperature and assumed to be constant over 0–t time interval. Hence, h_{tE} and h_{tW} have been considered constant over 0–t time interval.

After making above assumptions, Eq. (7) becomes first order simple differential equation. The solution of Eq. (7) with initial condition, $T_w = T_{w0}$ at $t = 0$, becomes:

$$Tw = \frac{\overline{f(t)}}{a}\left[1 - \exp(-a\Delta t)\right] + T_{w0}\exp(-a\Delta t) \tag{10}$$

The hourly yield can be found from equations as given below:

$$\dot{m}_E = \frac{\dot{q}_{ewE} \times 3600}{L} \tag{11a}$$

$$\dot{m}_W = \frac{\dot{q}_{ewW} \times 3600}{L} \tag{11b}$$

6. Results and discussion

The double slope solar still was tested during the month of October 2010 in the field conditions of Ghaziabad (28° 40′ N, 77° 25′ E), India. The typical experimental parameters recorded are illustrated in Table 2.

These values contain hourly data of solar intensity, temperatures namely ambient, water, inner and outer surface of glass cover, vapor temperature, distillate yield etc. The thermal model of double slope active solar still has been developed on the basis of energy balance of E-W condensing covers, water mass and basin liner. The climatic parameters such as ambient air temperature used in the modeling have been shown in Fig. 2a.

It increases from morning till afternoon hours and then starts decreasing. Fig. 2b shows the variation of solar intensity on condensing covers and at collector panels. The solar intensity incident on the east condensing cover is higher before 1:00 p.m. and lower in the after noon hours in comparison to the solar intensity on west condensing cover. The highest value of solar intensity at the east condensing cover was found to be 680 W m^{-2} at 12:00 noon whereas highest value of solar intensity at west condensing cover was 700 W m^{-2}

observed at 1:00 p.m. The standard values of design parameters used in the thermal modeling are given in Table 3.

By using the climatic, design parameters and heat transfer coefficient, the hourly variation of water, inner and outer condensing cover temperature and hourly yield have been evaluated. The various data obtained from thermal model are validated with experimental data. The closeness between theoretical and experimental data has been mentioned in terms of coefficient of correlation.

The expression for coefficient of correlation and root mean square percent deviation given by Chapra and Canale [17] are as follows:

$$r = \frac{N\sum X_iY_i - \sum(X_i)\sum(Y_i)}{\sqrt{N\sum X_i^2 - (\sum X_i)^2}\sqrt{N\sum Y_i^2 - (\sum Y_i)^2}} \tag{12}$$

The values of coefficient of correlation between theoretical and experimental results vary from 0.872 to 0.965.

The predicted values of hourly water temperature as have been compared with experimental result and are shown in Fig. 3. The coefficient of correlation between theoretical and experimental water temperature are found 0.935.

Hourly variation of theoretical and experimental inner glass covers temperature for E-W side of a double slope active solar still under forced circulation mode has been shown in Fig. 4.

From Fig. 4, it has been observed that the maxima of east condensing cover is lagging with the maxima of west inner condensing cover due to maximum solar intensity at E-W condensing cover at 13:00 and 14:00 h p.m. respectively. The coefficients of correlation between theoretical and experimental values for E-W inner condensing covers are 0.9231 and 0.9564 respectively. Similar observation can be made for outer glass cover temperature for double slope solar still.

Experimental and theoretical data for outer glass cover have been shown in Fig. 5 with correlation coefficient for E-W sides are 0.9440 and 0.9583 respectively.

The hourly variations in theoretical and experimental yield have been shown in Fig. 6.

In the morning the hourly yield for west condensing cover is more than east condensing cover. This may be due to cooled west condensing cover in comparison with east condensing cover. The same is true for afternoon hours. The overall results obtained from the present studies are quite similar to the results obtained by Dwivedi and Tiwari [1], Rubio et al. [3].

Table 2
Experimental observations for forced mode with FPCs connected in parallel for the typical day 5 October 2010 at 0.025 m water depth (50 kg water mass in basin)

| Time (h)	$I_s(t)_E$ (Wm⁻²)	$I_s(t)_W$ (Wm⁻²)	$I_c(t)$ (Wm⁻²)	T_a (°C)	T_v (°C)	T_b (°C)	T_w (°C)	T_{giE} (°C)	T_{giW} (°C)	T_{goE} (°C)	T_{goW} (°C)	m_{ewE} (kg)	m_{ewW} (kg)	V_{OC} (V)	I_{SC} (A)	V_L (V)	I_L (A)
7:00	0	0	0	23	21.5	21.5	22.1	20.4	20.3	20.9	21.6	0	0	–	–	–	–
8:00	260	160	240	26	27.9	27.2	26.6	25.1	24.9	26.6	25.9	0.014	0.018	–	–	–	–
9:00	360	280	420	28	39.8	30.1	35.5	34.5	33.2	33.3	30.4	0.01	0.03	19.2	1.2	9.9	0.9
10:00	580	460	620	29	45.3	34.6	44.1	39.6	37.9	36.3	34.5	0.095	0.113	19	1.7	15.1	1
11:00	680	520	720	31	49.4	38.7	53.1	46.5	43.7	44.1	40.8	0.199	0.28	18.4	2	16.3	1
12:00	680	660	780	33	53.1	50.3	61.2	50.9	48.8	48.6	46.3	0.333	0.375	18.1	2.2	17.3	1
13:00	660	700	740	34	59.7	53.9	66.3	56.1	57.4	54.1	55.6	0.549	0.568	17.1	1.9	15.8	1
14:00	500	620	640	34	58.9	57.2	66.2	53.3	56.1	49.6	55.2	0.685	0.672	17.9	1.7	15.3	1
15:00	300	480	460	33	56.6	60.6	63.9	51.7	54.2	48.5	53.1	0.491	0.48	18	1	12.4	0.8
16:00	180	320	300	32	50.3	58.2	54.4	48.6	49.3	45.4	47.7	0.42	0.396	–	–	–	–
17:00	120	200	160	31	44	47.5	45.6	42.4	43.6	39.3	42	0.246	0.204	–	–	–	–
18:00	0	0	0	30	33.9	35.6	35.3	32.8	32.9	31.2	32	0.213	0.193	–	–	–	–
19:00	0	0	0	30	26.2	27.9	28.2	25.9	26.1	25	25.1	0.137	0.154	–	–	–	–
20:00	0	0	0	29	25	26.5	26.8	24.6	24.8	24.1	24.3	0.056	0.059	–	–	–	–
21:00	0	0	0	28	24	24.5	25.1	23.9	23.2	23.2	22.9	0.049	0.05	–	–	–	–
22:00	0	0	0	27	23.2	24.1	24.3	22.7	22.9	22.4	22.5	0.043	0.046	–	–	–	–
23:00	0	0	0	26	22.7	23.5	23.6	22.6	22.7	22.4	22.4	0.034	0.039	–	–	–	–
0:00	0	0	0	25	22.6	23.1	23.3	22.6	22.6	22.4	22	0.031	0.032	–	–	–	–
1:00	0	0	0	25	22.5	22.7	23.1	22.4	22.5	22.2	21.3	0.025	0.029	–	–	–	–
2:00	0	0	0	24	22.3	22.5	22.6	22.2	22.1	22.1	20.4	0.024	0.028	–	–	–	–
3:00	0	0	0	23	21.8	22	22	19.8	19.6	19.8	19.5	0.024	0.025	–	–	–	–
4:00	0	0	0	22	21.7	22	21.8	18.7	18.8	18.6	18.6	0.011	0.01	–	–	–	–
5:00	0	0	0	22	21.6	21.9	21.5	18.1	18.2	18	18.5	0.008	0.01	–	–	–	–
6:00	0	0	0	22	21.4	21.8	21.4	17.9	18	17.8	18	0.008	0.008	–	–	–	–
7:00	0	0	0	23	22.2	22.2	21.9	20.8	21.7	21.1	22.1	0.008	0.008	–	–	–	–
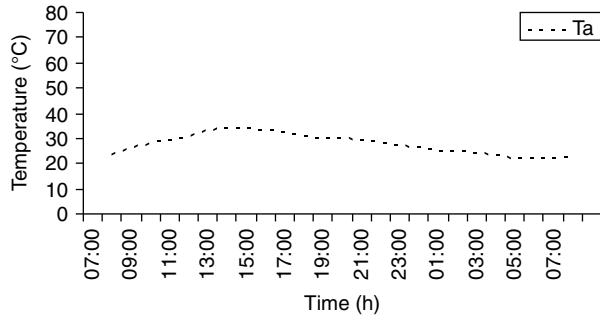
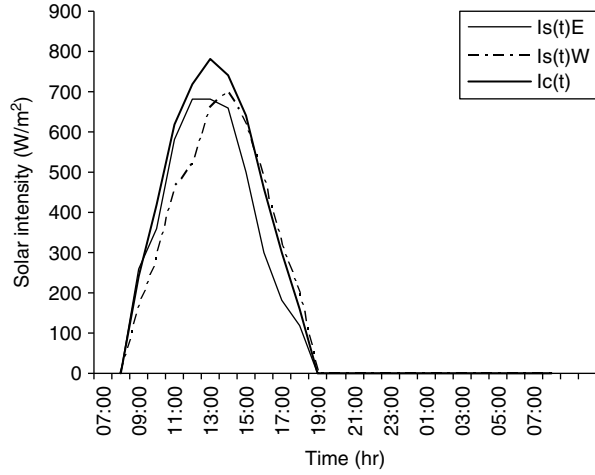Fig. 2a. Ambient air temperature during experiment.

Fig. 2b. Hourly variation of solar intensity on the collector panel and glass cover of solar still.

Table 3
The design parameters used in the thermal modeling

Parameters	Value
Design parameters for solar still	
α_b	0.85
α_g	0.06
α_w	0.7
ε_w	0.95
ε_g	0.95
Ag	1 m^2
L_b	0.005 m
L_g	0.004 m
K_b	0.035 W m^{-1} °C
K_g	0.780 W m^{-1} °C
C_W	4188 J kg^{-1} °C
M	50 kg
σ	5.67 × 10^{-8} W m^{-2} °C
Design parameters for flat plate collector	
Ac	4 m^2
F'	0.8
U_L	6 W m^{-2} °C
$(\alpha\tau)_c$	0.7
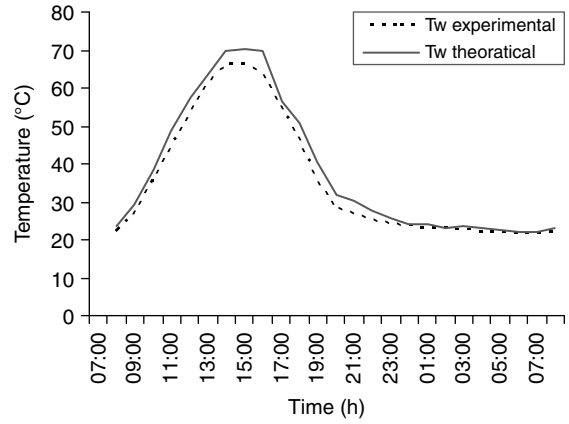
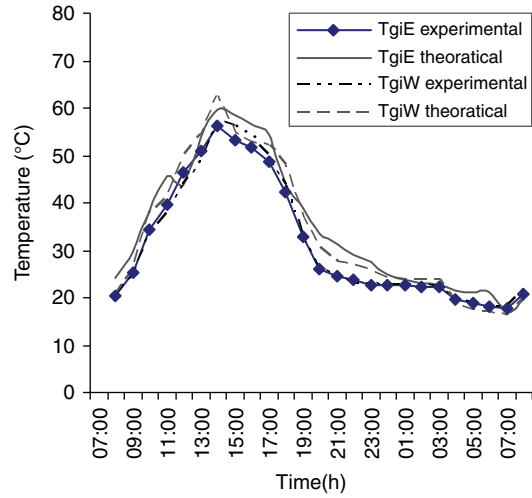Fig. 3. Hourly variation of theoretical and experimental water temperature.

Fig. 4. Hourly variation of theoretical and experimental inner condensing cover temperature for east and west side of double slope solar still.
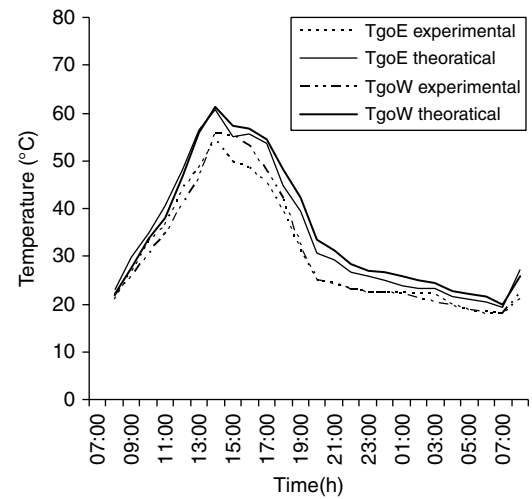

Fig. 5. Hourly variation of theoretical and experimental outer condensing cover temperature for east and west side of double slope solar still.
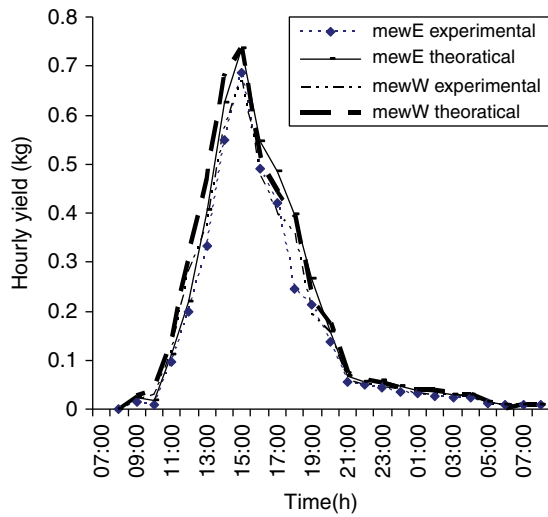
Fig. 6. Hourly variations of theoretical and experimental yields obtained from east and west side of HPVT double slope solar still.

7. Conclusions

In this paper mathematical model has been developed to study thermal asymmetries in double slope solar still. The developed model has been validated with experimental results. There are close agreement between theoretical and experimental results with coefficient of correlation varying from 0.872 to 0.965.

Symbols

A_b — area of basin, m^2
A_c — area of collector panel, m^2
A_g — area of condensing glass cover (m^2)
F' — flat plat collector efficiency factor
HPVT— hybrid photovoltaic thermal
h_1 — total internal heat transfer coefficient, $W\,m^{-2}\,°C$
h_{cw} — internal convective heat transfer coefficient, $W\,m^{-2}\,°C$
h_{ew} — internal evaporative heat transfer coefficient, $W\,m^{-2}\,°C$
h_{rw} — internal radiative heat transfer coefficient, $W\,m^{-2}\,°C$
h_o — heat transfer coefficient between outer condensing cover and ambient air, $W\,m^{-2}\,°C$
$I_s(t)$ — solar intensity on still glass covers, $W\,m^{-2}$
$I_c(t)$ — solar intensity on collector panels, $W\,m^{-2}$
k_g — thermal conductivity of condensing cover, $W\,m^{-1}\,°C$
L_g — thickness of condensing cover, m
L — latent heat of vaporization, $J\,kg^{-1}$
M — mass of water in the basin of solar still, kg

$\dot{m}$ — hourly distillate yield, $kg\,m^{-2}$
P — partial saturated vapor pressure, $N\,m^{-2}$
$\dot{Q}_U$ — useful thermal energy gain from the collector, $W\,m^{-2}$
$\dot{q}_{ew}$ — evaporative heat transfer rate, $W\,m^{-2}$
T_a — ambient air temperature, $°C$
T_b — basin liner temperature, $°C$
T_w — water temperature inside still, $°C$
T_v — vapor temperature inside still, $°C$
T_{gi} — inner glass covers temperature, $°C$
T_{go} — outer glass cover temperature, $°C$
U_L — overall heat transfer coefficient for flat plate collector, $W\,m^{-2}\,°C$
U_{EW} — internal radiative heat transfer coefficient between east and west condensing cover, $W\,m^{-2}\,°C$
U_{bw} — heat transfer coefficient between basin liner and water, $W\,m^{-2}\,°C$
U_{ba} — heat transfer coefficient between basin liner and ambient air, $W\,m^{-2}\,°C$
U_a — overall heat transfer coefficient between outer condensing cover and ambient air, $W\,m^{-2}\,°C$
V — air velocity, $m\,s^{-1}$

Subscripts

E — east side
W — west side
C — collector plate
w — water
gi — inner condensing cover
go — outer condensing cover
a — ambient
b — basin liner

References

[1] V.K. Dwivedi and G.N. Tiwari, Thermal modeling and carbon credit earned of a double slope passive solar still, Desalin. Water Treat., 3 (2010) 400–410.
[2] S. Kumar and A. Tiwari, An experimental study of hybrid photovoltaic thermal (PV/T) active solar still, Int. J. Energ. Res., 32 (2008) 847–858.
[3] E. Rubio, L.J. Fernandez and A. Miguel Porta-Gandara, Modeling thermal symmetries in double slope solar stills, Renew. Energ., 29 (2004) 895–906.
[4] A.K. Tiwari and G.N. Tiwari, Annual performance analysis and thermal modeling of passive solar still for different inclination of condensing cover, Int. J. Energ. Res., 31(14) (2007) 1358–1382.
[5] H. Tanaka, T. Nosoko and T. Nagata, A highly productive basin type multiple effect coupled solar still, Desalination, 130 (2000) 279–293.
[6] R. Tripathi and G.N. Tiwari, Effect of water depth on internal heat and mass transfer for active solar distillation, Desalination, 173 (2005) 187–200.

[7] G.N. Tiwari, V. Dimri, U. Singh, A. Chel and B. Sarkar, Comparative thermal performance evaluation of an active solar distillation system, IJER, 31 (2007) 1465–1482.

[8] V.K. Dwivedi and G.N. Tiwari, Experimental validation of thermal model of a double slope active solar still under natural circulation mode, Desalination, 250 (2010) 49–55.

[9] I.A. Hayek and O. Badran, The effect of using different designs of solar stills on water distillation, Desalination, 169 (2004) 121–127.

[10] O.O. Badran and H.A. Al-Tahaineh, The effect of coupling flat plate collector on the solar still productivity, Desalination, 183 (2004) 137–142.

[11] E. Rubio, M.A. Porta and J.L. Fernandez, Cavity geometry influence on mass flow rate for single and double slope solar stills, Appl. Energ, 20 (2000) 1105–1111.

[12] S. Kumar and G.N. Tiwari, Life cycle cost analysis of single slope hybrid (PV/T) active solar still, Appl. Energ, 86 (2009) 1995–2004.

[13] V.K. Dwivedi and G.N. Tiwari, Comparison of internal heat transfer coefficients in passive solar stills by different thermal models: An experimental validation, Desalination, 246 (2009) 304–318.

[14] R. Dev and G.N. Tiwari, Characteristic equation of a hybrid (PV-T) active solar still, Desalination, 254(4) (2010) 126–137.

[15] R. Dev, H.N. Singh and G.N. Tiwari, Characteristic equation of double slope passive solar still, Desalination, 267 (2010) 261–266.

[16] R. Dev and G.N. Tiwari, Chapter 6-solar distillation, In: Ray C, Jain R (eds.), Drinking water treatment: strategies for sustainability, 1st Ed., DOI 10.1007/978-94-007-1104-4_6, Springer Science, Business Media BV, (2011) 163–165.

[17] S.C. Chapra and R.P. Canale, Numerical Methods for Engineer, McGraw-Hill, New York, 1989.

Appendix-1

$$p = U_1 . U_2 - U_{EW}^2 . A_{gE} . A_{gW}$$

$$A_1 = R_1 . U_2 + R_2 . U_{EW} . A_{gE}$$

$$A_2 = h_{1wE}.A_b.U_2 + h_{1wW}.A_b.U_{EW}.A_{gE}$$

$$B_1 = R_1.U_{EW}.A_{gW} + R_2.U_1$$

$$B_2 = h_{1wE}.A_b.U_{EW}.A_{gW} + h_{1wW}.A_b.U_1$$

$$R_1 = \alpha'_g.I_s \left(t \right)_E .A_{gE} + h_{go}.A_{gE}.T_a$$

$$R_2 = \alpha'_g.I_s \left(t \right)_W .A_{gW} + h_{go}.A_{gW}.T_a$$

$$U_1 = h_{1wE}.A_b + U_{EW}.A_{gE} + h_{go}.A_{gE}$$

$$U_2 = h_{1wW}.A_b + U_{EW}.A_{gW} + h_{go}.A_{gW}$$

Appendix-2

Heat transfer relationship used in thermal modeling: Heat transfer equations used in the thermal modeling are as given below:

1. External heat transfer coefficient

Heat transfer from glass cover to ambient air takes place by convection and radiation. The total heat transfer coefficient from glass cover to ambient is given by:

$$h_{aE} = h_{aW} = 5.7 + 3.8 \, V$$

The overall heat transfer coefficient from basin to ambient is given by the equation:

$$U_{ba} = \cfrac{1}{\cfrac{L_b}{K_b} + \cfrac{1}{h_b}}$$

2. Internal heat transfer coefficient

The convection, evaporation and radiation are the mode of heat transfer from water mass to inner glass cover. Dunkle's equation for convective heat transfer coefficient is:

$$h_{cW} = 0.884 \left[T_w - T_{giE} + \frac{(P_w - P_{giE})T_w}{268.9 \times 10^3 - P_w} \right]^{\frac{1}{3}}$$

and, evaporative heat transfer coefficient is given by:

$$h_{ew} = 16.276 \times 10^{-3} h_{cwE} \frac{P_w - P_{giE}}{T_w - T_{giE}}$$

Radiative heat transfer coefficient is calculated by:

$$h_{rw} = \frac{\sigma(T_w^2 + T_{giE}^2)(T_w + T_{giE})}{\cfrac{1}{\varepsilon_w} + \cfrac{1}{\varepsilon_g} - 1}$$

Radiative heat transfer between E-W surface has also been considered. The radiative heat transfer coefficient between two glass surfaces is given by:

$$U_{EW} = 0.034\sigma \left[(T_{giE} + 273)^2 + (T_{giW} + 273)^2 \right]$$
$$\times \left[T_{giE} + T_{giW} + 546 \right]$$

The evaporative heat transfer rate from E-W side of a double slope solar still is also given by:

$$\dot{q}_{ewE} = h_{ewE}(T_w - T_{giE})$$

and

$$\dot{q}_{ewW} = h_{ewW}(T_w - T_{giW})$$